J. Mech. Phys. Solids Vol. 40, No. 2, pp. 393–416, 1992.
Printed in Great Britain.

0022–5096/92 $5.00 + 0.00

INTERFACIAL CRACK-TIP FIELD IN ANISOTROPIC ELASTIC SOLIDS

H. GAO, M. ABBUDI and D. M. BARNETT
Division of Applied Mechanics, Stanford University, Stanford, CA 94305, U.S.A.

(*Received* 22 *January* 1991)

ABSTRACT

FOR INTERFACIAL cracks in anisotropic elastic solids, controversies exist in that several different definitions for the crack-tip field have been proposed in the literature. In this paper, we first devise a novel and convenient scheme for constructing the interfacial crack fields and then carry out a mismatch analysis for understanding the oscillatory structure of the crack-tip stress singularity. It is hoped that the mismatch analysis can shed some light on the controversial issues from a different perspective. Among different definitions for the stress intensity factors, it is found that the solution proposed by WU [*Int. J. Solids Struct.* **27**, 455 (1991)], which conforms to a general definition suggested by RICE [*J. appl. Mech.* **55**, 98 (1988)], is consistent with the analysis of local interface mismatch near the crack tip. Critical quantities governing the oscillation and mismatch are numerically evaluated for a number of materials including two fiber-reinforced composites and a group of crystals of cubic symmetry.

INTRODUCTION

DUE TO the wide application of composite materials in recent years, there has been a great interest in understanding the behavior of cracks along an interface between dissimilar elastic solids. The interface cracks are peculiar in that they may exhibit the so-called oscillatory behavior near the crack tip (WILLIAMS, 1959); it has been found that, under general anisotropic conditions, the stress field behaves as $r^{-1/2+i\varepsilon}$ at distance r from the crack tip, ε being a bimaterial constant referred to as the oscillation index. Despite such complications as the oscillatory displacement field predicting interpenetration (contact) of the crack faces behind the crack tip, it has been argued [e.g. RICE (1988) and RICE *et al.* (1990)] that the solutions can still be used to characterize the interface fracture process since the contact zone size is found to be extremely small (e.g. subatomic) for a broad range of bimaterial and loading configurations of practical importance. RICE (1988) suggested that the crack-tip field be normalized such that the traction at a characteristic distance $\hat{r}$ along the interface ahead of the crack tip is given by

$$\mathbf{t} = \frac{\mathbf{k}}{\sqrt{2\pi\hat{r}}}, \tag{1}$$

where the vector

$$\mathbf{k}^T = \{K_{II}, K_I, K_{III}\} \tag{2}$$

defines the interfacial mode "I, II, III" stress intensity factors having the conventional dimensions of $FL^{-3/2}$. As discussed by Rice, the length parameter $\hat{r}$ may be chosen arbitrarily as long as it is held fixed when specimens of a given material pair but with different loading and geometry conditions are compared. Different values of $\hat{r}$ will not alter the magnitude of $\mathbf{k}$ but will change its phase angle. It is helpful to visualize the parameter $\hat{r}$ as a representative scale of the "fracture process zone" for a given bimaterial combination. Once $\hat{r}$ is fixed, $\mathbf{k}$ can be used to characterize the interface fracture toughness. Since interface fracture is inherently mixed mode with $\mathbf{k}$ having three scalar components, the interface toughness is usually defined by a failure locus in the 3-space spanned by K_I, K_{II} and K_{III}, which gives the critical magnitude of the vector $\mathbf{k}$ as a function of the two orientation angles of $\mathbf{k}$.

Interfacial cracks in anisotropic materials have been discussed by many authors [e.g. WU (1990, 1991), QU and LI (1991), NI and NEMAT-NASSER (1991), SUO (1990), BASSANI and QU (1989), TEWARY *et al.* (1989), TING (1986, 1990), CLEMENTS (1971), WILLIS (1971) and GOTOH (1967)]. Among those authors, Willis, Suo, Qu and Li, and Wu have attempted to define stress intensity factors for the crack-tip singularity. However, important controversies seem to exist in that several different solutions have been proposed and each has a different definition for the stress intensity factors. WILLIS (1971) derived a solution for the near-tip field which is scaled by a complex valued "stress concentration factor". SUO (1990) followed a similar procedure to that used by Willis, but defined a different set of stress intensity factors. QU and LI (1991) adopted Willis's approach to the interfacial crack fields by considering a distribution of interfacial dislocations, but they gave another definition for the stress intensity factors which do not have the conventional dimension. Those solutions are obviously correct, but do not appear to be fully consistent with the definition in (1). Most recently, WU (1990, 1991) has shown that, when the characteristic length $\hat{r}$ is introduced, WILLIS's (1971) original solution can be converted into a form such that the traction $t_j = \sigma_{2j}$ along the interface ahead of the crack tip is

$$\mathbf{t} = \frac{1}{\sqrt{2\pi r}} \mathbf{R}\left[\left(\frac{r}{\hat{r}}\right)^{i\varepsilon}\right] \mathbf{k}, \tag{3}$$

where $\mathbf{R}[\ ]$, defined such that $\mathbf{R}[1] = \mathbf{I}$, is a real and non-dimensional matrix function to be given in (56). The stress intensity factors defined by (3) are consistent with (1) and the elastic solutions associated with this definition appears to be more explicit than those given by other authors. The oscillation index ε is typically very small [e.g. HUTCHINSON (1990)], so that the variable quantity $(r/\hat{r})^{i\varepsilon} = \exp[i\varepsilon \ln(r/\hat{r})]$ and the matrix function $\mathbf{R}$ appearing in (3) have only a weak variation with r. This has been used as a justification for the interfacial crack modes defined in the spirit of (1) (RICE *et al.*, 1990).

In an earlier study on interfacial cracks in isotropic elastic materials, GAO (1991) has analyzed the crack-tip oscillation from the fundamental viewpoint of the interface mismatch that results from cracking. In that work, the interface mismatch is assessed using the surface Green's function tensor (SGF) of a homogeneous solid and represented by a distribution of dislocations whose superposed effect leads to the crack-tip

oscillation. It has been shown that the interface mismatch affects the interface crack field in two ways. First, the near-tip oscillation arises due to the local mismatch at the crack tip. Second, the mismatch on the global scale affects the stress intensity factor of the oscillatory singularity field. For interface cracks in anisotropic elastic solids, the crack-tip field could also be related to the interface mismatch ahead of the crack tip. It is hoped in this paper that the mismatch analysis can perhaps help to identify or justify a proper definition for the interfacial crack-tip field from a different perspective. Indeed, we find that the solution given by WU (1990, 1991), which conforms to Rice's general definition in (1), is consistent with the mismatch analysis near the crack tip. The original derivation procedure of Wu appears to be rather cumbersome. We give an alternative, but perhaps more straightforward scheme for constructing the interfacial crack fields. Our method can be more easily extended to more complex stress singularity analyses such as interfacial cracks in anisotropic materials with coupled fields, e.g. piezoelectric, magnetostrictive solids, etc. Finally, to provide some more insight into the interfacial fracture in anisotropic materials, the oscillation index ε is numerically evaluated for the case of two bonded solids reinforced by unidirectional fibers with fiber directions misoriented across the interface plane; also, it is demonstrated, by example using a group of crystals of cubic symmetry, that quantities which govern the interface mismatch can be conveniently expanded into a Fourier series with only a few significant terms.

COMPLEX VARIABLE REPRESENTATIONS

Stroh formalism

For convenience we briefly review some elements of the two-dimensional anisotropic elasticity theory. With respect to a fixed Cartesian coordinate system x_i ($i = 1, 2$ or 3), the equilibrium equation can be written as

$$\sigma_{ij,i} = 0, \tag{4}$$

where σ_{ij} are stress components which are related to the displacement field u_k by the generalized Hooke's law

$$\sigma_{ij} = C_{ijkl} u_{k,l}. \tag{5}$$

Here C_{ijkl} is the elastic moduli tensor and the comma denotes differentiation. The summation convention will always apply to repeated Latin indices but not to repeated Greek indices.

The solution to a class of anisotropic problems in which the deformation field is independent of the x_3-coordinate was first considered by ESHELBY *et al.* (1953). In that case, (4) becomes

$$\sigma_{1j,1} + \sigma_{2j,2} = 0, \tag{6}$$

and the stresses may be expressed in terms of three potential functions $\varphi_j(x_1, x_2)$ by

$$\sigma_{1j} = -\varphi_{j,2}, \quad \sigma_{2j} = \varphi_{j,1}. \tag{7}$$

Consider the following basic solution form

$$u_i = a_i f(z), \quad \varphi_i = l_i f(z), \quad z = x_1 + p x_2, \tag{8}$$

where f is an arbitrary function and a_i, l_i and p are complex-valued constants. By Hooke's law it may be verified that the two vectors a_i and l_i are related by

$$l_i = [C_{i2j1} + pC_{i2j2}]a_j. \tag{9}$$

It was shown by STROH (1958, 1962) and INGEBRIGTSEN and TONNING (1969), that the constants p, a_i and l_i may be simultaneously determined from the six-dimensional eigenvalue problem

$$\mathbf{N}\xi = p\xi, \tag{10}$$

where ξ is a six-dimensional vector

$$\xi^T = (a_1, a_2, a_3, l_1, l_2, l_3) \tag{11}$$

and $\mathbf{N}$ is a real 6×6 matrix

$$\mathbf{N} = \begin{bmatrix} -\mathbf{T}^{-1}\mathbf{R}^T & \mathbf{T}^{-1} \\ \mathbf{R}\mathbf{T}^{-1}\mathbf{R}^T - \mathbf{Q} & -\mathbf{R}\mathbf{T}^{-1} \end{bmatrix}. \tag{12}$$

Here $(\ )^T$ denotes matrix transposition and the 3×3 matrices $\mathbf{T}$, $\mathbf{R}$ and $\mathbf{Q}$ are defined as

$$(\mathbf{Q})_{ik} = C_{i1k1}, \quad (\mathbf{R})_{ik} = C_{i1k2}, \quad (\mathbf{T})_{ik} = C_{i2k2}. \tag{13}$$

Bold letters will be used exclusively for vectors, tensors and matrices. The eigenvalue problem (10) leads to six eigenvalues p_α ($\alpha = 1, 2, \ldots, 6$) associated with six eigenvectors $a_{i\alpha}$ and $l_{i\alpha}$ which are normalized by

$$\xi_\alpha^T \mathbf{J} \xi_\beta = \delta_{\alpha\beta} \quad (\alpha \text{ and } \beta = 1, \ldots, 6), \tag{14}$$

where $\delta_{\alpha\beta}$ is the Kronecker delta and $\mathbf{J}$ is a 6×6 matrix

$$\mathbf{J} = \begin{bmatrix} \mathbf{0} & \mathbf{I} \\ \mathbf{I} & \mathbf{0} \end{bmatrix}, \quad \text{where} \quad \mathbf{I} = \begin{bmatrix} 1 & 0 & 0 \\ 0 & 1 & 0 \\ 0 & 0 & 1 \end{bmatrix}. \tag{15}$$

A straightforward numerical computation can be performed to solve for p_α, $a_{i\alpha}$ and $l_{i\alpha}$ without regard to boundary conditions. The positive definiteness of the strain energy function requires that the six p_α form three complex conjugate pairs (ESHELBY *et al.*, 1953). We shall arrange the eigenvalues so that the first three p_α have positive imaginary parts and also

$$p_{\alpha+3} = \bar{p}_\alpha, \quad a_{i,\alpha+3} = \bar{a}_{i\alpha}, \quad l_{i,\alpha+3} = \bar{l}_{i\alpha} \quad \text{for} \quad \alpha = 1, 2 \text{ and } 3, \tag{16}$$

where an overbar denotes complex conjugation. With this arrangement two 3×3 matrices $\mathbf{A}$ and $\mathbf{L}$ will be defined as having components $a_{i\alpha}$ and $l_{i\alpha}$ with indices i and α both ranging over 1–3.

Surface impedance tensor $\mathbf{Z}$ *and surface admittance tensor* $\mathbf{Y}$

It looks as if the linear relation (9) between the Stroh eigenvectors $l_{i\alpha}$ and $a_{i\alpha}$ should depend on the eigenmode α since p_α does. However, INGEBRIGTSEN and TONNING (1969) have shown that relation (9) can be replaced by a linear connection which is independent of α, namely,

$$l_{i\alpha} = iZ_{ij}a_{j\alpha}, \tag{17}$$

where $\mathbf{Z}$ is a positive definite and hermitian matrix which obeys the second-order tensor transformation rule under coordinate rotations in the x_1–x_2 plane; it has been referred to as the surface impedance tensor measuring the material stiffness in the 1–2 plane. BARNETT (1985) has shown that $\mathbf{Z}$ is convenient for use in problems involving dislocations and cracks along an interface. Important properties of $\mathbf{Z}$ were investigated in sufficient detail by BARNETT and LOTHE (1985) to facilitate the analysis of surface (Rayleigh) wave and interfacial (Stoneley) wave problems. In terms of the 3×3 matrices $\mathbf{A}$ and $\mathbf{L}$, one may write

$$\mathbf{Z} = -i\mathbf{L}\mathbf{A}^{-1}, \quad \mathbf{Y} = \mathbf{Z}^{-1} = i\mathbf{A}\mathbf{L}^{-1}, \tag{18}$$

where the inverse matrix $\mathbf{Y}$, referred to as the surface admittance tensor, measures the compliance of the material. The hermitian property

$$\mathbf{Z} = \bar{\mathbf{Z}}^T, \quad \mathbf{Y} = \bar{\mathbf{Y}}^T \tag{19}$$

indicates that the real parts Re [$\mathbf{Z}$] and Re [$\mathbf{Y}$] are symmetric real matrices while the imaginary parts Im [$\mathbf{Z}$] and Im [$\mathbf{Y}$] are anti-symmetric real matrices.

Field representation via a complex potential function

A more general solution can be constructed by a linear superposition of all the eigenmode solutions. Since the eigenmodes $\alpha = 4$–6 are conjugate to the first three modes, as shown in (16), one may write this solution in the form

$$u_i = \mathrm{Re}\left[\sum_{\alpha=1}^{3} a_{i\alpha}d_\alpha f(z_\alpha)\right], \quad \varphi_i = \mathrm{Re}\left[\sum_{\alpha=1}^{3} l_{i\alpha}d_\alpha f(z_\alpha)\right], \tag{20}$$

where $z_\alpha = x_1 + p_\alpha x_2$ and d_α are unknown constant coefficients to be determined from the boundary conditions. To simplify the expressions, the following convention will be adopted: if $\mathbf{q}$ is a vector and $\mathbf{Q}$ is a matrix, then the notations $\mathbf{q} * f(z)$ and $\mathbf{Q} * f(z)$ *always* imply that

$$\mathbf{q} * f(z) = \mathbf{L}\boldsymbol{\Lambda}[f(z)]\mathbf{L}^{-1}\mathbf{q}, \quad \mathbf{Q} * f(z) = \mathbf{L}\boldsymbol{\Lambda}[f(z)]\mathbf{L}^{-1}\mathbf{Q},$$
$$\boldsymbol{\Lambda}[f(z)] = \mathrm{diag}\,[f(z_1), f(z_2), f(z_3)], \tag{21}$$

where diag [ ] denotes a diagonal matrix. With these notations, we introduce a vector complex potential function

$$\mathbf{\Phi}(z) = \mathbf{q} * f(z), \tag{22}$$

where $\mathbf{q} = \mathbf{Ld}$, $\mathbf{d}$ being the unknown coefficient vector d_α ($\alpha = 1, 2$ or 3) appearing in (20). The displacement equation in (20) may then be written as

$$\mathbf{u} = \mathrm{Im}\,[\mathbf{Y}\mathbf{\Phi}(z)]. \tag{23}$$

The stress functions are written as $\varphi_j = \mathrm{Re}\,[\Phi_j(z)]$ so that

$$\sigma_{2j} = \mathrm{Re}\,[\Phi_{j,1}(z)], \quad \sigma_{1j} = -\mathrm{Re}\,[\Phi_{j,2}(z)]. \tag{24}$$

In this representation, the problem of solving (4) and (5) has been reduced to one of finding the complex function $\mathbf{\Phi}(z)$ from the boundary conditions, similar to the corresponding complex representation in isotropic elasticity.

The resultant traction on an arbitrary curve from point A to point B, lying in the x_1–x_2 plane with normal $\mathbf{n}$, is given by

$$p_j = \int_A^B \sigma_{ij} n_i \,\mathrm{d}s = -\int_A^B \mathrm{Re}\,[\Phi_{j,i}(z)]\,\mathrm{d}x_i = \mathrm{Re}\,[\Phi_j(A)] - \mathrm{Re}\,[\Phi_j(B)]. \tag{25}$$

The Airy stress function considered by BACON *et al.* (1979) is equivalent to $-\mathrm{Re}\,[\mathbf{\Phi}(z)]$ in our current notation.

One may further verify the following useful operational relations pertaining to convention (21): letting $\mathbf{P}$ be a 3×3 matrix and $\mathbf{q}$ be a 3×1 vector, one may verify that

(i) $\mathbf{Pq} * f(z) \neq (\mathbf{Pq}) * f(z)$, $\mathbf{PQ} * f(z) \neq (\mathbf{PQ}) * f(z)$.

(ii) $\mathbf{q} * [f(z) + g(z)] = \mathbf{q} * f + \mathbf{q} * g$, $\mathbf{Q} * [f(z) + g(z)] = \mathbf{Q} * f + \mathbf{Q} * g$.

(iii) $[\mathbf{Q} * f(z)]\mathbf{q} = (\mathbf{Qq}) * f(z)$, $[\mathbf{Q} * f(z)]\mathbf{P} = (\mathbf{QP}) * f(z)$.

(iv) $[\mathbf{q} * f(z)] * g(z) = \mathbf{q} * (fg)$, $[\mathbf{Q} * f(z)] * g(z) = \mathbf{Q} * (fg)$.

(v) $\mathbf{q} * f(z)|_{x_2 = 0} = \mathbf{q} f(x_1)$, $\mathbf{Q} * f(z)|_{x_2 = 0} = \mathbf{Q} f(x_1)$.

Relation (v) follows from the fact that the eigenvector matrix $\mathbf{L}$ and its inverse cancel one another in (21) when $x_2 = 0$ {in which case $\mathbf{\Lambda}[f(x_1)] = \mathbf{I} f(x_1)$}.

Bimaterial constants

For bimaterial problems the following matrices will be frequently used:

$$\begin{aligned} \mathbf{M} &= \mathbf{Y}_1 + \bar{\mathbf{Y}}_2 = \mathbf{D} - i\mathbf{W}, \\ \mathbf{N} &= (\mathbf{Y}_1 + \bar{\mathbf{Y}}_2)^{-1} = \tilde{\mathbf{D}} - i\tilde{\mathbf{W}}, \end{aligned} \tag{26}$$

where subscripts 1 and 2 refer to materials 1 and 2, and $\mathbf{D}$, $\mathbf{W}$, $\tilde{\mathbf{D}}$ and $\tilde{\mathbf{W}}$ are real matrices related by

$$\tilde{\mathbf{W}}\tilde{\mathbf{D}}^{-1} = -\mathbf{D}^{-1}\mathbf{W}, \quad \tilde{\mathbf{D}}^{-1} = \mathbf{W}\mathbf{D}^{-1}\mathbf{W} + \mathbf{D}. \tag{27}$$

Observe that $\mathbf{D}$ and $\tilde{\mathbf{D}}$ are symmetric and positive definite while $\mathbf{W}$ and $\tilde{\mathbf{W}}$ are anti-symmetric.

Dislocations along an interface

As a preliminary application, consider a dislocation of Burgers vector **b** and a force **p** at an interface between materials 1 and 2. The solution of $\boldsymbol{\Phi}(z)$ has the following logarithmic functional form

$$\boldsymbol{\Phi}(z) = \begin{cases} \mathbf{q}_1 * \ln z & \text{in material 1} \\ \mathbf{q}_2 * \ln z & \text{in material 2} \end{cases} \tag{28}$$

with a branch cut along the negative x_1-axis. The continuity of the traction σ_{2j} across the interface and the equilibrium of the total resultant force on a closed curve surrounding the origin require

$$\mathrm{Re}\,[\mathbf{q}_1] = \mathrm{Re}\,[\mathbf{q}_2], \quad -\mathrm{Re}\,[\pi i(\mathbf{q}_1 + \mathbf{q}_2)] = -\mathbf{p}. \tag{29}$$

Compatibility requires that the displacement field is continuous across the interface along the positive x_1-axis while discontinuously changing by **b** across the branch cut along the negative x_1-axis, i.e.

$$\mathrm{Im}\,[\mathbf{Y}_1\mathbf{q}_1] = \mathrm{Im}\,[\mathbf{Y}_2\mathbf{q}_2], \quad \mathrm{Im}\,[\pi i(\mathbf{Y}_1\mathbf{q}_1 + \mathbf{Y}_2\mathbf{q}_2)] = \mathbf{b}. \tag{30}$$

Equations (29) and (30) yield the final solution

$$\mathbf{q}_1 = \frac{1}{\pi}\mathbf{N}(\mathbf{b} - i\overline{\mathbf{Y}}_2\mathbf{p}), \quad \mathbf{q}_2 = \frac{1}{\pi}\mathbf{N}(\mathbf{b} - i\overline{\mathbf{Y}}_1\mathbf{p}), \tag{31}$$

which is consistent with the earlier result of BARNETT and LOTHE (1974) and BARNETT (1985). The self-energy of an interface dislocation is obtained by an integration along the cut surface along $x_1 < 0$ as

$$U^{\mathrm{int}} = \frac{1}{2}\int_{-r^0}^{-R} \sigma_{2j} b_j \, \mathrm{d}x_1 = \frac{1}{2}\int_{-r^0}^{-R} \mathrm{Re}\,[\mathbf{b}^T\boldsymbol{\Phi}_{,1}]\,\mathrm{d}x_1 = \frac{1}{2\pi}\mathbf{b}^T\tilde{\mathbf{D}}\mathbf{b}\ln\frac{R}{r^0}, \tag{32}$$

where R is the dimension of the field and r^0 the dislocation core cut-off. It is useful to note that the tensor $\tilde{\mathbf{D}}$ is just the well-known prelogarithmic energy factor matrix of a dislocation lying along the interface.

INTERFACIAL CRACK-TIP FIELD

Singularity eigenmodes

Consider a crack along an interface between two anisotropic materials (1 and 2), as shown in Fig. 1. Let the potential function

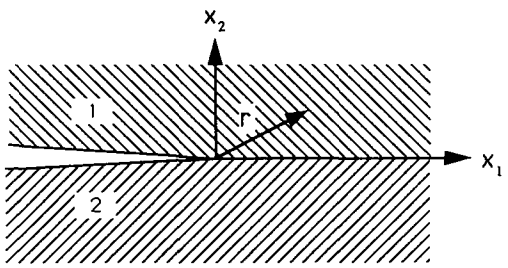

FIG. 1. Interface crack between two dissimilar anisotropic materials.

$$\mathbf{\Phi}_1(z) = \mathbf{q} * z^{1/2+i\delta} \tag{33}$$

represent the crack-tip singularity field within material region 1, where $\mathbf{q}$ and δ are complex-valued constants to be determined. The traction continuity across the interface plane $x_2 = 0$ requires that the potential function in material 2 be accordingly given by

$$\mathbf{\Phi}_2(z) = \bar{\mathbf{q}} * z^{1/2-i\bar{\delta}}. \tag{34}$$

As discussed by WILLIS (1971) and TING (1986), the type of solutions for which the displacements are continuous across the bonded portion of the interface ($x_1 > 0$, $x_2 = 0$) and the tractions vanish along the crack faces must satisfy the eigenvalue equation

$$(\mathbf{N} - e^{-2\pi\delta}\bar{\mathbf{N}})\mathbf{q} = 0. \tag{35}$$

Define an eigenvalue constant

$$\lambda = (1 - e^{-2\pi\delta})/(1 + e^{-2\pi\delta}) = \tanh(\pi\delta) \tag{36}$$

and a mismatch matrix

$$\mathbf{P} = -\mathbf{D}^{-1}\mathbf{W} = \tilde{\mathbf{W}}\tilde{\mathbf{D}}^{-1}, \tag{37}$$

where $\mathbf{D}$, $\mathbf{W}$, $\tilde{\mathbf{D}}$ and $\tilde{\mathbf{W}}$ have been defined in (26). With these matrices, it can be shown that the eigenvalue equation (35) possesses the following alternative forms

$$(\tilde{\mathbf{W}} + i\lambda\tilde{\mathbf{D}})\mathbf{q} = 0, \tag{38}$$

$$(\mathbf{W} - i\lambda\mathbf{D})\mathbf{q} = 0, \tag{39}$$

$$\mathbf{P}\mathbf{q} = -i\lambda\mathbf{q}. \tag{40}$$

In particular, (40) suggests that the eigenvalues $-i\lambda$ can be solved from the mismatch matrix $\mathbf{P}$. TING (1986) has obtained the characteristic equation for (35), which may be written in the form

$$\lambda(\lambda - \beta)(\lambda + \beta) = 0, \tag{41}$$

where

$$\beta = \sqrt{-\frac{1}{2}\operatorname{tr}(\mathbf{P}^2)}. \tag{42}$$

The three eigenvalues

$$\lambda_1 = 0, \quad \lambda_2 = \beta, \quad \lambda_3 = -\beta \tag{43}$$

lead to three eigenmodes for the allowable crack-tip stress singularities $r^{-1/2+i\delta_\alpha}$, namely

$$\delta_1 = 0, \quad \delta_2 = \varepsilon, \quad \delta_3 = -\varepsilon, \tag{44}$$

where the oscillation index ε is determined from

$$\varepsilon = \frac{1}{2\pi}\ln\frac{1+\beta}{1-\beta} = \frac{1}{\pi}\tanh^{-1}\beta. \tag{45}$$

Crack-tip field

Recently, WU (1990, 1991) has shown that WILLIS's (1971) original solution for the crack-tip field can be converted into a form consistent with Rice's definition in (1). Wu's derivation procedure appears to be rather cumbersome and his results are not given in the most convenient form. In the following, we shall give an alternative, but perhaps more straightforward scheme for constructing the interfacial crack fields. It is worth mentioning that our method may be easily extended to more complex stress singularity analyses such as interfacial cracks in anisotropic materials with coupled fields.

We shall construct the crack-tip field by superposing the singularity eigenmodes given in (33) and (44). It is well known (Cayley–Hamilton theorem) that the mismatch matrix $\mathbf{P}$ must satisfy its own characteristic equation (41), namely

$$\mathbf{P}(\mathbf{P}+i\beta\mathbf{I})(\mathbf{P}-i\beta\mathbf{I}) = 0. \tag{46}$$

This means that if we define matrices

$$\mathbf{Q}_1 = \mathbf{P}^2+\beta^2\mathbf{I}, \quad \mathbf{Q}_2 = \mathbf{P}(\mathbf{P}-i\beta\mathbf{I}), \quad \mathbf{Q}_3 = \mathbf{P}(\mathbf{P}+i\beta\mathbf{I}), \tag{47}$$

then, for each singularity mode λ_α, $\mathbf{Q}_\alpha$ satisfies

$$\mathbf{P}\mathbf{Q}_\alpha = -i\lambda_\alpha\mathbf{Q}_\alpha. \tag{48}$$

Thus, all the column vectors in $\mathbf{Q}_\alpha$ are eigenvectors pertaining to the eigenmode λ_α. One can also prove the following orthogonality relations

$$\mathbf{Q}_\alpha^T\mathbf{D}\mathbf{Q}_\beta = 0 \tag{49}$$

for all α and $\beta = 1, 2$ or 3 except that

$$\mathbf{Q}_1^T\mathbf{D}\mathbf{Q}_1 = \beta^2\mathbf{D}\mathbf{Q}_1, \quad \mathbf{Q}_3^T\mathbf{D}\mathbf{Q}_2 = (\mathbf{Q}_2^T\mathbf{D}\mathbf{Q}_3)^T = -2\beta^2\mathbf{D}\mathbf{Q}_2, \tag{50}$$

where, in deriving (50), it is helpful to use (48) with the relation $\mathbf{P}^T\mathbf{D} = -\mathbf{D}\mathbf{P}$.

Equation (48) suggests that a more general eigenvector associated with the eigenmode λ_α may be written as

$$\mathbf{q}_\alpha = c_\alpha\mathbf{Q}_\alpha\mathbf{k}, \tag{51}$$

where c_α is a scalar and $\mathbf{k}$ is a real vector. Superposing all the singularity modes, the crack-tip field in material 1 can be constructed as

$$\mathbf{\Phi}_1(z) = \left(\sum_{\alpha=1}^{3} c_\alpha\mathbf{Q}_\alpha * z^{1/2+i\delta_\alpha}\right)\mathbf{k}, \tag{52}$$

where $\mathbf{k}$ will be taken as the stress intensity factor for the interfacial crack. The unknown constants c_α must satisfy

$$c_1 = \bar{c}_1, \quad c_2 e^{-\pi\varepsilon} = \bar{c}_3 e^{\pi\varepsilon} \tag{53}$$

for tractions to vanish along the crack faces. Now imposing Rice's definition, namely,

requiring that the traction at a characteristic distance $\hat{r}$ along the interface ahead of the crack tip be given in the form of (1), we easily determine c_α as

$$c_1 = \frac{2}{\sqrt{2\pi\beta^2}}, \quad c_2 = -\frac{e^{\pi\varepsilon}\hat{r}^{-i\varepsilon}}{\sqrt{2\pi}(1+2i\varepsilon)\beta^2\cosh(\pi\varepsilon)},$$
$$c_3 = -\frac{e^{-\pi\varepsilon}\hat{r}^{i\varepsilon}}{\sqrt{2\pi}(1-2i\varepsilon)\beta^2\cosh(\pi\varepsilon)}. \tag{54}$$

The crack-tip field given by (47), (52) and (54) is consistent with the corresponding solutions derived in WU (1991) using a different approach. Compared to Wu's derivation, our method is more convenient, perhaps even more so when more complex stress singularity analyses are encountered. For example, KUO and BARNETT (1991) have recently found that interfacial cracks in piezoelectric materials have four allowable singularity eigenmodes, with the possibility of having two distinct oscillation index. In that case and others, the crack-tip field will still be given in a form similar to (52), with the eigenvector matrices $\mathbf{Q}_\alpha$ obtained from factorization of the characteristic equation and the unknown constants c_α determined by conforming the field to Rice's definition in (1).

Following the full solution (52), the traction along the interface at any distance r ahead of the crack tip can be obtained as

$$\mathbf{t} = \mathrm{Re}\left[\sum_{\alpha=1}^{3}(1/2+i\delta_\alpha)c_\alpha\mathbf{Q}_\alpha r^{-1/2+i\delta_\alpha}\right]\mathbf{k} = \mathbf{R}\left[\left(\frac{r}{\hat{r}}\right)^{i\varepsilon}\right]\frac{\mathbf{k}}{\sqrt{2\pi r}}, \tag{55}$$

where the matrix function

$$\mathbf{R}[c] = \mathrm{Re}\left[(\mathbf{Q}_1 - \mathbf{Q}_2 c)/\beta^2\right] \tag{56}$$

has previously appeared in (3). It is elementary to verify that $\mathbf{R}[1] = \mathbf{I}$ so that (55) is consistent with the general definition in (1).

According to (34), the field solution in material 2 should be derived from

$$\mathbf{\Phi}_2(z) = \left(\sum_{\alpha=1}^{3}\bar{c}_\alpha\bar{\mathbf{Q}}_\alpha * z^{1/2-i\tilde{\delta}_\alpha}\right)\mathbf{k}. \tag{57}$$

Using the displacement representation (23), one may further show that the crack face relative displacement vector at distance r behind the crack tip is

$$\Delta\mathbf{u}(r) = \left(\sum_{\alpha=1}^{3}c_\alpha\mathbf{D}\mathbf{Q}_\alpha e^{-\pi\delta_\alpha}r^{1/2+i\delta_\alpha}\right)\mathbf{k}. \tag{58}$$

Energy release rate

The asymptotic solutions given in (55) and (58) can be used to calculate the crack-tip energy release rate G by the standard procedure of crack closure, i.e.

$$G = \frac{1}{2\Delta}\int_0^{\Delta} \mathbf{t}^T(r)\Delta\mathbf{u}(\Delta - r)\,\mathrm{d}r. \tag{59}$$

Substituting (55) and (58) into (59) and using the orthogonality relations derived in (49) and (50) lead to

$$G = \frac{1}{4}\mathbf{k}^T\tilde{\mathbf{D}}^{-1}\mathbf{k}, \tag{60}$$

where the matrix $\tilde{\mathbf{D}}^{-1}$ is just the inverse of the dislocation energy factor matrix $\tilde{\mathbf{D}}$ in (32). Equation (60) has been derived by Wu (1991); it extends a well-known relation between the crack-tip energy release rate and the dislocation energy factor matrix (Barnett and Asaro, 1972) to interfacial cracks in anisotropic materials. The corresponding energy release rate expressions in Willis (1971), Suo (1990) and Qu and Li (1991) do not seem to show similar relations to the dislocation energy factor matrix. This is perhaps because their definitions for the crack-tip field are not fully compatible with (1).

A finite interface crack

Consider a finite interface crack of length l subjected to crack face loading $\mathbf{t}_2^{\infty}$ (Fig. 2), corresponding to the reduced problem of remote loading. The form of the near-tip asymptotic field (52) suggests that the solution has the form

$$\mathbf{\Phi}_1(z) = \left\{\sum_{\alpha=1}^{3} d_\alpha \mathbf{Q}_\alpha * [(z-l)^{1/2+i\delta_\alpha} z^{1/2-i\delta_\alpha} - z]\right\}\mathbf{t}_2^{\infty} \tag{61}$$

in material region 1, and the form

$$\mathbf{\Phi}_2(z) = \left\{\sum_{\alpha=1}^{3} \bar{d}_\alpha \bar{\mathbf{Q}}_\alpha * [(z-l)^{1/2-i\bar{\delta}_\alpha} z^{1/2+i\bar{\delta}_\alpha} - z]\right\}\mathbf{t}_2^{\infty} \tag{62}$$

in material 2. The unknown constants d_α are determined by requiring that the crack face traction

$$\mathbf{t} = \mathrm{Re}\left[\frac{\partial \mathbf{\Phi}_1(x_1)}{\partial x_1}\right] = -\mathbf{t}_2^{\infty} \tag{63}$$

along $0 < x_1 < l$, giving

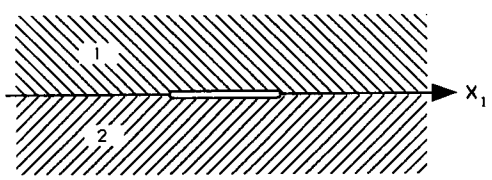

Fig. 2. Finite interface crack.

$$d_1 = \frac{1}{\beta^2}, \quad d_2 = -\frac{e^{\pi\varepsilon}}{2\beta^2 \cosh(\pi\varepsilon)}, \quad d_3 = -\frac{e^{-\pi\varepsilon}}{2\beta^2 \cosh(\pi\varepsilon)}. \tag{64}$$

Using the basic definition in (1), the stress intensity factor for the finite crack is given by

$$\mathbf{k} = \mathrm{Re}\left[\sum_{\alpha=1}^{3} d_\alpha \mathbf{Q}_\alpha (1+2i\delta_\alpha)\left(\frac{\hat{r}}{l}\right)^{i\delta_\alpha}\right]\mathbf{t}^\infty \sqrt{\pi l/2}. \tag{65}$$

The crack-tip energy release rate may be evaluated by substituting (65) into (60).

Analysis of Interface Mismatch

In the above section, we have discussed the basic solution for the interfacial crack-tip field in anisotropic materials by WU (1990, 1991), and we have given a more convenient derivation procedure. Since solutions with different definitions have been proposed in the literature, it seems necessary to provide further justification for the definition we have adopted. For that purpose, we shall approach the problem from a different perspective by recognizing that the crack-tip oscillation arises due to the interface mismatch that results from cracking. The previous analysis of GAO (1991) on the mismatch of interfacial cracks in isotropic materials will be extended to the anisotropic case. It is hoped that the mismatch analysis can perhaps shed some light on the controversies in the literature.

SGF tensor

The fact that the basic interface crack configurations shown in Figs 1 and 2 may be viewed as the interaction between two dissimilar homogeneous half-planes via distributed forces along their surfaces suggests an approach to examining interface crack fields via properties of the SGF tensor $\mathbf{G}$ of each homogeneous half-plane. By definition, the tensor $\mathbf{G}$ allows one to use a simple superposition procedure to write the displacement response $\mathbf{u}(x_1)$ along the surface $x_2 = 0$ due to an arbitrary distribution of surface traction $\mathbf{t}(x_1')$ in the convolution form

$$\mathbf{u}(x_1) = \int_{-\infty}^{\infty} \mathbf{G}(x_1 - x_1')\mathbf{t}(x_1')\,\mathrm{d}x_1'. \tag{66}$$

The tensor $\mathbf{G}$ was first derived by BARNETT and LOTHE (1975) and it can be written in our current notation as

$$\mathbf{G} = \mathbf{G}^S + \mathbf{G}^A, \tag{67}$$

where

$$\mathbf{G}^S = -\frac{1}{\pi}\mathrm{Re}[\mathbf{Y}]\ln|x_1 - x_1'|, \quad \mathbf{G}^A = \frac{1}{2}\mathrm{Im}[\mathbf{Y}]\,\mathrm{sgn}(x_1 - x_1'). \tag{68}$$

Applying Betti's reciprocal theorem

$$\mathbf{G}(x_1 - x_1') = \mathbf{G}^T(x_1' - x_1) \tag{69}$$

to $\mathbf{G}^S$ and $\mathbf{G}^A$ simply leads to the hermitian property of the tensor $\mathbf{Y}$.

When the 1–2 plane is a mirror plane, there is a simple geometrical interpretation for the anti-symmetric tensor $\mathbf{G}^A$. In that case, the in-plane and the out-of-plane deformations decouple, leading to

$$\mathbf{G}^A = \frac{1}{2}\,\mathrm{Im}\,[\mathbf{Y}]\,\mathrm{sgn}\,(x_1 - x_1'), \quad \text{where} \quad \mathrm{Im}\,[\mathbf{Y}] = \begin{bmatrix} 0 & d & 0 \\ -d & 0 & 0 \\ 0 & 0 & 0 \end{bmatrix}, \tag{70}$$

where d is a real constant. This corresponds to a uniform lateral expansion along the surface of magnitude $d/2$ about a normal force and an anti-symmetric warp of the same magnitude about a shear force. The value of d is independent of the crystal orientation below because Im [**Y**] given in (70) is invariant to the tensor transformations under coordinate rotations in the 1–2 plane.

Interface mismatch

To understand the interface crack problem described in Fig. 3(a), consider the corresponding homogeneous crack configuration in Fig. 3(b) with a distribution of traction along the crack faces. We assume that the crack face traction is of induced type, i.e. equal in magnitude but opposite in sense on the upper and lower crack faces.

Now imagine that the homogeneous body in Fig. 3(b) is separated without relaxation into two half-planes along the x_1-axis. Along the separated surface, a distribution of traction $\mathbf{t}(x_1')$ would be found which is independent of the material moduli. For the prescribed crack face traction, both the potential function $\mathbf{\Phi}(z)$ and the crack plane traction are independent of the moduli (BARNETT and ASARO, 1972). Let the

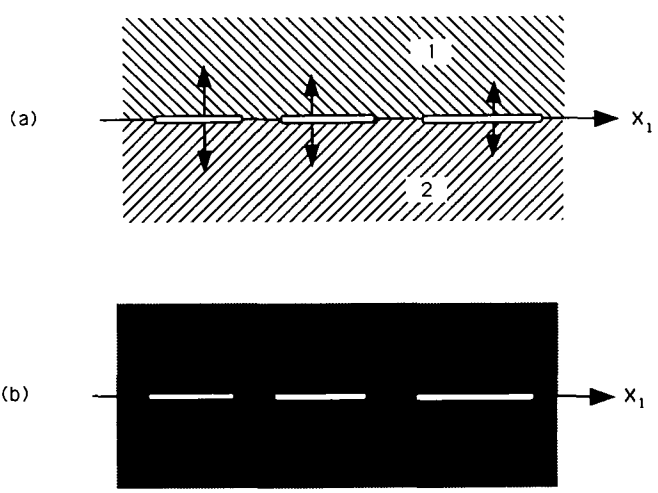

FIG. 3. (a) Collinear interface cracks, and (b) corresponding homogeneous cracks.

coordinate origin be set at an arbitrarily chosen crack tip. Then, relative to the chosen crack tip, the traction $\mathbf{t}(x_1')$ results in a displacement along the surface according to

$$\mathbf{u}(x_1) = \int_{-\infty}^{\infty} [\mathbf{G}(x_1 - x_1') - \mathbf{G}(-x_1')]\mathbf{t}(x_1')\,dx_1'. \tag{71}$$

In particular, the symmetric tensor $\mathbf{G}^S$ results in a contribution

$$\mathbf{u}^S(x_1) = -\frac{1}{\pi}\mathrm{Re}[\mathbf{Y}]\int_{-\infty}^{\infty}\mathbf{t}(x_1')\ln\left|\frac{x_1 - x_1'}{x_1'}\right|dx_1'. \tag{72}$$

The fact that $\mathbf{t}(x_1')$ is independent of the material moduli leads to the conclusion that $\mathbf{u}^S(x_1)$ must be identically zero along the uncracked portions. This is because, if we specialize (72) to the isotropic case, symmetry requires that the integral involved in (72) vanish everywhere except along the crack faces (e.g. mode I symmetry requires the displacement u_2 to vanish accordingly).

The anti-symmetric tensor $\mathbf{G}^A$ also results in a surface deformation

$$\mathbf{u}^A(x_1) = \frac{1}{2}\mathrm{Im}[\mathbf{Y}]\int_{-\infty}^{\infty}\mathbf{t}(x_1')[\mathrm{sgn}(x_1 - x_1') - \mathrm{sgn}(-x_1')]\,dx_1' = \mathrm{Im}[\mathbf{Y}]\int_0^{x_1}\mathbf{t}(x_1')\,dx_1'. \tag{73}$$

Since $\mathbf{u}^S$ is identically zero along the uncracked portions, the only mismatch arising in the process of joining an upper half-plane 1 with a lower half-plane 2 to form an interface crack is the difference in $\mathbf{u}^A$, i.e.

$$[\![\mathbf{u}(x_1)]\!] = (\mathbf{u}^A)_2 - (\mathbf{u}^A)_1 = \mathbf{W}\int_0^{x_1}\mathbf{t}(x_1')\,dx_1'. \tag{74}$$

The interface mismatch and oscillation vanish when (74) does. The condition

$$\mathbf{W} = [\![\mathrm{Im}[\mathbf{Y}]]\!] = 0 \tag{75}$$

has been referred to as the non-oscillation condition for the bimaterial. An exception is that when the crack face traction $\mathbf{t}$ has the same orientation as the axial vector of the anti-symmetric matrix $\mathbf{W}$, i.e. $\mathbf{Wt} = 0$, in which case the oscillation vanishes even if $\mathbf{W} \neq 0$. For general crack face tractions, condition (75) ensures that there is no interface mismatch, so that no extra forces will be needed to form the interface crack. This means that the stress state in half-planes 1 and 2 remains identical to that of the corresponding homogeneous cracks. The case of bulk loading can be reduced to crack face tractions by superposition. Hence, as discussed by SUO (1990), for collinear cracks in an infinite bimaterial body the deformation field will remain identical to that of the corresponding homogeneous problem if the induced crack face tractions are independent of the material moduli. An obvious example is a finite crack subjected to remote stresses, in which case the induced crack face traction is indeed moduli-independent and the stress field is identical to that of the corresponding homogeneous crack problem. This can be directly verified from (61). Further, when the oscillation vanishes, the following two important observations can be made by examining (55), (58) and (60): (i) the near-tip stress field decouples into the classical form $\mathbf{t} = \mathbf{k}/\sqrt{2\pi r}$ everywhere along the interface ahead of the crack tip, and (ii) the crack face

relative displacement $\Delta\mathbf{u}$ and the energy release rate G become the average of the corresponding homogeneous solutions for materials 1 and 2.

The above mismatch analysis indicates that, for interface cracks in an infinite body subjected to prescribed crack face traction, the oscillation and mismatch are equivalent in that the mismatch vanishes when oscillation does, and vice versa. This is not true for interfacial cracks involving more complicated loadings and/or finite geometries such as thin films on a substrate. For those problems, the presence of an interface can strongly alter the stress intensity factor even when the oscillation index ε vanishes. For isotropic interface cracks, HUTCHINSON (1990) has reviewed some of the recent results of the stress intensity factors for various fracture specimens. Based on those calculations, Hutchinson proposed to ignore the oscillation effects by setting $\varepsilon = 0$ in many engineering applications, provided that in those cases the effect of ε is much less significant compared to that of the external loading and geometry.

When $[\![\text{Im}\,[\mathbf{Y}]]\!] \neq 0$, the existing interface mismatch (74) can be represented by a distribution of mismatch dislocations along the interface, with dislocation density given by

$$\partial[\![\mathbf{u}(x_1)]\!]/\partial x_1 = \mathbf{W}\mathbf{t}(x_1). \tag{76}$$

The non-oscillation condition

For a general anisotropic material, the in- and anti-plane deformations are coupled to each other so that the tensor non-oscillation condition (75) actually corresponds to three scalar conditions. The tensor property of $\mathbf{W} = \text{Im}\,[\mathbf{Y}_2 - \mathbf{Y}_1]$ suggests that, for two materials with a fixed relative orientation, ε is invariant under the rotation of the interface in the 1–2 plane (TING, 1986, 1990). Also, for a material with the 1–2 plane as a mirror plane, in which case Im [**Y**] is proportional to a scalar d given in (70), the fact that the value of d is independent of the in-plane crystal orientation suggests that, if the oscillation vanishes for one relative crystal orientation, it will also vanish for any other interfaces for which the crack front is a zonal axis (QU and BASSANI, 1989; BASSANI and QU, 1989).

Crack-tip oscillation vs local mismatch

When the non-oscillation condition (75) is violated, oscillation at an interfacial crack tip would occur as a consequence of the interface mismatch. The general relation (76) between the mismatch and traction along the interface can be used to form an iteration procedure that adjusts an initially assumed traction distribution $\mathbf{t}(x_1)$ to the oscillatory state. In that procedure, the mismatch due to the initial $\mathbf{t}(x_1)$ is represented by an array of dislocations with density given in (76), but the superposed effect of such mismatch dislocations will change the traction $\mathbf{t}(x_1)$ itself, forming a loop adjustment between the traction and mismatch along the interface. It will be shown below that this procedure leads to the oscillatory singularity field given by (52).

Set the coordinate origin at a chosen crack tip. The mismatch dislocation density along the interface ahead of the crack tip is related to the traction there by (76). Use

the non-oscillatory field as the initial state in the loop adjustment procedure described above, so that the traction is taken as $\mathbf{t}(x_1) = \mathbf{k}/\sqrt{2\pi x_1}$ and

$$\partial[\![\mathbf{u}(x_1)]\!]/\partial x_1 = \mathbf{W}\mathbf{k}/\sqrt{2\pi x_1}. \tag{77}$$

To assess the effect of such dislocations, we need the formulae for a single Volterra dislocation interacting with an interface crack under the non-oscillatory condition. This issue has been addressed in SUO (1990). For a semi-infinite interface crack with tip at the coordinate origin interacting with a dislocation at $x_1 = t$ ahead of the crack tip, the stress intensity factors and the potential function are given by

$$\mathbf{k} = -\frac{2\mathbf{D}^{-1}\mathbf{b}}{\sqrt{2\pi t}}, \quad \mathbf{\Phi}_{,1}(z) = (\mathbf{D}^{-1}\mathbf{b}) * \left[\frac{1}{\pi(z-t)}\sqrt{\frac{t}{z}}\right]. \tag{78}$$

The superposed effect of the mismatch dislocations in (77) within the crack-tip region characterized by $\hat{r}$ can be calculated using the single dislocation formula (78), which modifies the crack-tip field in material 1 to

$$\begin{aligned}\mathbf{\Phi}_{,1}(z) &= \mathbf{k} * \frac{1}{\sqrt{2\pi z}} - \int_0^{\hat{r}} \left[\mathbf{D}^{-1}\frac{\partial[\![\mathbf{u}(t)]\!]}{\partial t}\right] * \left[\frac{1}{\pi(z-t)}\sqrt{\frac{t}{z}}\right] \mathrm{d}t \\ &= \left[\mathbf{k} + \varepsilon \mathbf{P}\mathbf{k} * \left(\ln\frac{z}{\hat{r}} - \pi i\right)\right] * \frac{1}{\sqrt{2\pi z}} + 0(\varepsilon^2),\end{aligned} \tag{79}$$

where the approximation $\varepsilon = \beta/\pi$ (correct to second order in β) has been used and quantities of order $z/\hat{r}$ are ignored in the present "near-tip" calculation.

At a fixed position z, one may expand the exact solution of $\mathbf{\Phi}_{,1}(z)$, given by (52), into a power series in ε as

$$\mathbf{\Phi}_{,1}(z) = \left[\mathbf{k} + \varepsilon \mathbf{P}\mathbf{k} * \left(\ln\frac{z}{\hat{r}} - \pi i\right) + \frac{\varepsilon^2}{2}\mathbf{P}^2\mathbf{k} * \ln\frac{z}{\hat{r}}\left(\ln\frac{z}{\hat{r}} - 2\pi i\right)\right] * \frac{1}{\sqrt{2\pi z}} + 0(\varepsilon^3). \tag{80}$$

It can be observed that the result (79) of the first adjustment from the non-oscillatory state gives the first-order expansion in ε of the oscillatory field. Using the first-order potential given in (79) to update the traction distribution $\mathbf{t}(x_1)$ by (24) and repeating the above adjustment procedure result in the second-order expansion expression of $\mathbf{\Phi}_{,1}(z)$, as expressed in (80). Continuing the adjustment procedure leads to a Taylor expansion series in ε of the oscillatory field at any given material point. Summation of such a Taylor expansion then constructs the full oscillatory near-tip field given in (52). Therefore, the crack-tip field given in (52), which conforms to Rice's general definition in (1) for the interfacial stress intensity factors, is consistent with the analysis of interface mismatch at the crack tip.

Global mismatch effect

The presence of interface mismatch not only alters the nature of the singularity at a crack tip as we have explored, but also changes the singularity strength of the oscillatory field. To understand how interface mismatch affects the stress intensity factor $\mathbf{k}$, consider, for example, a semi-infinite crack subjected to a pair of crack face forces $\pm\mathbf{f}$ at a distance l behind the crack tip. In that case, Wu (1990) has obtained the exact solution as

$$\mathbf{k} = \sqrt{\frac{2}{\pi l}}\mathbf{R}\left[\cosh \pi\varepsilon\left(\frac{\hat{r}}{l}\right)^{i\varepsilon}\right]\mathbf{f}, \tag{81}$$

where the matrix function $\mathbf{R}$ has been given in (56). For a fixed $\hat{r}/l$, the above may be expanded into a Taylor power series in ε as

$$\mathbf{k} = \sqrt{\frac{2}{\pi l}}\left(\mathbf{I}+\varepsilon\mathbf{P}\ln\frac{\hat{r}}{l}\right)\mathbf{f}+0(\varepsilon^2), \tag{82}$$

where the zeroth-order term $\mathbf{f}\sqrt{2/\pi l}$ corresponds to the solution of the non-oscillatory state. The first-order term can be understood as the superposed effect of mismatch dislocations given by (76) with traction $\mathbf{t}(x_1)$ taken as the $\varepsilon = 0$ result, i.e.

$$\frac{\partial[\![\mathbf{u}(x_1)]\!]}{\partial x_1} = \frac{\mathbf{W}\mathbf{f}}{\pi(x_1+l)}\sqrt{\frac{l}{x_1}}. \tag{83}$$

Since the above dislocation density is of order ε, we may use the non-oscillatory crack-dislocation formula (78) in the superposition procedure. Thus, the mismatch dislocations outside the crack-tip region characterized by $\hat{r}$ give the first-order term in (82):

$$\mathbf{k} = \frac{2\mathbf{D}^{-1}}{\sqrt{2\pi}}\int_{\hat{r}}^{\infty}\frac{1}{\sqrt{x_1}}\left[\frac{\partial[\![\mathbf{u}(x_1)]\!]}{\partial x_1}\right]dx_1 = \sqrt{\frac{2}{\pi l}}\varepsilon\mathbf{P}\mathbf{f}\ln\frac{\hat{r}}{l}. \tag{84}$$

As explained before, the traction and mismatch along the interface will adjust themselves to the oscillatory state via the loop procedure based on (76), eventually resulting in the full Taylor expansion of the exact $\mathbf{k}$-solution (81). Clearly, the length $\hat{r}$ is acting here as a characteristic distance at the crack tip where the global information of geometry and loading is transmitted to the fracture process zone.

As a brief summary of this section, we have extended the mismatch analysis of Gao (1991) for isotropic materials to the anisotropic case, and have shown that the oscillatory field solution given in (52) is consistent with the mismatch analysis. This part of the work is mainly motivated by the fact that several different definitions for the interfacial stress intensity factors exist in the literature. The authors hope that the mismatch analysis provides a different perspective for the interface crack problems and perhaps sheds some light on the existing controversies regarding the interfacial crack-tip field.

NUMERICAL EXAMPLES

Fiber-reinforced composite materials

To provide some more insight into the mismatch and oscillation at interfacial crack tips, we have considered two bonded semi-infinite media (epoxy), each reinforced by unidirectional fibers parallel to the interface plane with the fiber directions misoriented by an angle γ across the interface. Right-hand orthonormal triads $X_i(1)$ and $X_i(2)$ are attached to the upper (1) and lower (2) half-spaces, respectively, so that the X_1-axis is in the fiber direction and the X_2-axis is normal to the interface. Assume that the fiber distances are negligible compared to other length scales, so that the composite can be treated as being homogeneous and transversely isotropic. Two important cases have been studied: (i) a half space of graphite–epoxy (material 1) bonded to one of glass–epoxy (material 2), and (ii) both materials 1 and 2 of graphite–epoxy with fiber directions misoriented across the interface. The selected graphite–epoxy composite is reinforced by IM6 carbon fibers with elastic constants (in unit of GPa): $c_{11} = 207.693$, $c_{22} = c_{33} = 15.192$, $c_{12} = c_{13} = 7.334$, $c_{23} = 7.726$, $c_{44} = 3.733$, $c_{55} = c_{66} = 8.40$; the glass–epoxy has elastic constants $c_{11} = 40.964$, $c_{22} = c_{33} = 11.535$, $c_{12} = c_{13} = 4.564$, $c_{23} = 6.022$, $c_{44} = 2.756$, $c_{55} = c_{66} = 4.140$ (TSAI, 1989).

The coordinates x_i are attached to sample the possible cracking orientations. The x_3-axis is chosen to be always parallel to the crack front and the x_2-axis coincides with the interface normal, i.e. the X_2-axis. The x_1-axis lies in the interface plane with an angle θ relative to the $X_1(1)$ direction. As θ increases, the x_i-coordinate frame is rotated about the X_2-axis, sampling all possible crack orientations. The coordinate frames in the interface plane are shown in Fig. 4. We examine the variation of the oscillation index ε as a function of the crack orientation angle θ at each chosen fiber misorientation angle γ.

The results of ε vs θ are plotted in Fig. 5 as dotted lines for case (i) (graphite–glass) and as solid lines for case (ii) (graphite–graphite) for $\gamma = 0$, 45, 60 and 90°. Since ε is periodic in θ with period of π, only the range $0 < \theta < \pi$ is displayed. The following observations can be made from the numerical results. (a) In all cases, ε is a small parameter less than 0.05. (b) For each chosen γ, ε varies with θ in an undulating manner. There exist multiple crack orientations for which ε attains a local maximum or minimum. (c) The maximum value of ε increases with the fiber misorientation angle γ for the graphite–graphite system but not for graphite–glass system. (d) The

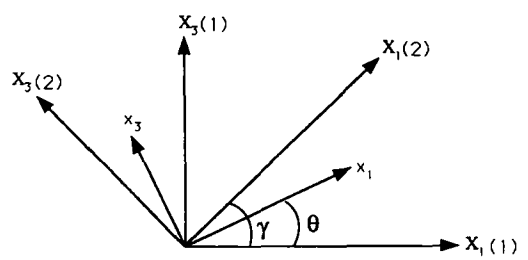

FIG. 4. Coordinate frames in the interface plane of two fiber-reinforced composites. Fiber directions are in the $X_1(1)$ and $X_1(2)$ directions, and the x_3-axis denotes the orientation of an interfacial crack front.

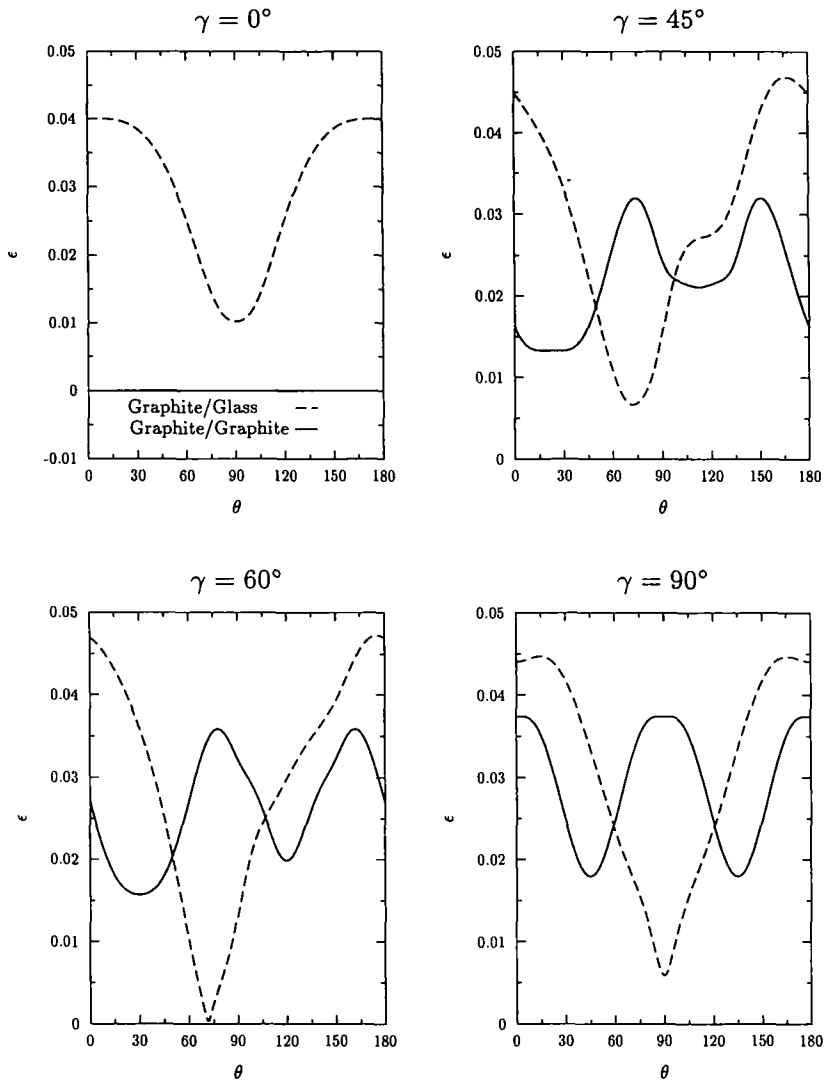

FIG. 5. Oscillation index ε vs crack orientation angle θ for bonded composites with fiber directions misoriented by γ across the interface plane.

graphite–glass system involves a larger variation of ε than graphite–graphite (a more homogeneous system). (e) We have discovered a non-oscillatory state for the graphite–glass system, i.e. ε vanishes when $\gamma = 60^\circ$ and $\theta = 72^\circ$.

The interface fracture toughness is a function of the phase angle of the local crack tip loading configuration which is weakly affected by ε [e.g. RICE *et al.* (1989)]. Assume that all the conditions along the crack front are uniform if $\varepsilon = 0$, such as a remotely loaded penny-shape crack. It is then foreseeable that due to the existing effect of ε the crack front may tend to grow into a somewhat polygonal shape on which ε is

distributed more uniformly, with the orientation of each polygon side minimizing (or maximizing) $\varepsilon(\theta)$.

Cubic crystals

Equations (73) and (74) have suggested that the interface mismatch is governed by the difference in the tensor Im [**Y**] for both materials. In the calculations to follow, we show that Im [**Y**] can be conveniently expanded into a Fourier series as a function of the crack orientation relative to the fixed crystal orientations in the interface plane. We examine the behavior of Im [**Y**] for a number of selected crystals of cubic symmetry on different crystal plane orientations.

The orthonormal triad X_i is attached to a chosen crystal plane such that the plane normal is in the X_2-direction. Similarly, the coordinate frame x_i is employed to represent the crack orientations. The x_2-axis coincides with the X_2-axis and the x_3-axis is parallel to the crack front. As the angle θ between x_1 and X_1 varies from 0 to 2π, the x_3-axis is rotated in the x_1–x_3 plane about the plane normal (X_2), screening all possible cracking orientations. The tensor Im [**Y**] in the rotating x_i frame, as a function of θ, is expanded into a Fourier series

$$\text{Im}\,[\mathbf{Y}(\theta)] = \mathbf{U}^{(0)} + \sum_{n=1}^{\infty} \mathbf{U}^{(n)} \cos n\theta + \sum_{n=1}^{\infty} \mathbf{V}^{(n)} \sin n\theta. \tag{85}$$

The Fourier coefficients $\mathbf{U}^{(n)}$ and $\mathbf{V}^{(n)}$ are real and anti-symmetric matrices. The first coefficient $\mathbf{U}^{(0)}$, as the mean value of Im [**Y**] over $0 < \theta < 2\pi$, has only two non-vanishing components, $U_{21}^{(0)} = -U_{12}^{(0)}$, i.e.

$$\mathbf{U}^{(0)} = \begin{bmatrix} 0 & U_{12}^{(0)} & 0 \\ -U_{12}^{(0)} & 0 & 0 \\ 0 & 0 & 0 \end{bmatrix}. \tag{86}$$

For isotropic materials, all the higher-mode Fourier coefficients vanish and $U_{12}^{(0)} = (1-2\nu)/2\mu$, where μ and ν are the shear modulus and Poisson's ratio, respectively.

Values of the coefficients $\mathbf{U}^{(n)}$ and $\mathbf{V}^{(n)}$ are computed for materials Al, Na, Nb and Ni on plane orientations (010), (110) and (111). Table 1 displays the value of $U_{12}^{(0)}$ for different materials and for different plane orientations along with the isotropic

TABLE 1. *Comparison of* $\hat{U}_{12}^{(0)}$ *with the isotropic case for different crack plane orientations*

Material	A	$1-2\nu/2\mu$	(010)	(110)	(111)
Al	1.21	0.0577	0.0585	0.0582	0.0581
Na	8.15	0.7868	0.8051	0.7654	0.7427
Nb	0.51	0.0273	0.0267	0.0271	0.0272
Ni	2.52	0.0236	0.0241	0.0234	0.0231

approximation $(1-2\nu)/2\mu$ when ν and μ are taken as the Voigt average elastic constants (HIRTH and LOTHE, 1982). It is found that the isotropic estimate from Voigt average constants is a very good approximation for materials of cubic symmetry. The relative error ranges from less than 1.5% for Al, the most isotropic material in the group, to less than 5% for Na, the most anisotropic material in the group. Tables 2–4 give the non-vanishing components in the higher-order coefficients $\mathbf{U}^{(n)}$ and $\mathbf{V}^{(n)}$. In Table 2, the X_1- and X_3-axes have been taken along the $\langle 100\rangle$ and $\langle 001\rangle$ directions. In Table 3, the X_1- and X_3-axes coincide with the $\langle 1\bar{1}0\rangle$ and $\langle 001\rangle$ directions. Finally,

TABLE 2. *Crack plane is the* (010) *crystal plane*

Material	n	$\hat{\mathbf{U}}_{12}^{(n)}$	n	$\hat{\mathbf{V}}_{23}^{(n)}$
Al	0	0.058548	0	0.002122
Na	0	0.805135	4	0.447968
	4	0.083465	8	−0.109433
	8	0.054218	12	0.026453
Nb	0	0.026720	4	−0.004045
	4	−0.000520	8	−0.000719
Ni	0	0.024137	4	0.003675
	4	0.001059	8	−0.000677

TABLE 3. *Crack plane is the* (110) *crystal plane*

Material	n	$\hat{\mathbf{U}}_{12}^{(n)}$	n	$\hat{\mathbf{V}}_{23}^{(n)}$
Al	0	0.058228	2	0.001044
			4	0.001441
Na	0	0.765433	2	0.183152
	2	0.044649	4	0.110741
	4	0.075568	6	0.082947
	6	0.027518	8	−0.038742
	8	0.020342	12	0.018118
Nb	0	0.027090	2	−0.002080
	2	−0.000585	4	−0.003947
	4	−0.000347	8	−0.000476
Ni	0	0.023402	2	0.001650
	2	0.000905	4	0.001531
	4	0.000865	6	0.000493

TABLE 4. *Crack plane is the* (111) *crystal plane*

Material	n	$\hat{\mathbf{U}}_{12}^{(n)}$	n	$\hat{\mathbf{V}}_{13}^{(n)}$	n	$\hat{\mathbf{V}}_{23}^{(n)}$
Al	0	0.058121	3	0.001921		
Na	0	0.742752	3	0.293570	6	−0.253510
	6	0.037623	9	0.042153	12	0.011216
Nb	0	0.027220	3	−0.004194	6	−0.001256
Ni	0	0.023136	3	0.002713	6	−0.001407

in Table 4, the X_1- and X_3-axes lie along the $\langle 11\bar{2}\rangle$ and $\langle 1\bar{1}0\rangle$ directions. The coefficients smaller than 1% of the mean value $U_{12}^{(0)}$ have been neglected.

The numerical results reveal that the tensor Im [**Y**] can be conveniently expanded into a Fourier series, and in all cases studied only a few significant coefficients are involved. For Al, the most isotropic material in the group, the second Fourier coefficient is already smaller than 4% of the mean value $U_{12}^{(0)}$. For the other two materials, Nb and Ni, with anisotropy factor equal to 0.51 and 2.52, Im [**Y**] exhibits only a minor fluctuation of approximately 15% about the mean value. The most anisotropic material in the group, Na, has a variation of about 40% about the mean. Thus, the mismatch between cubic materials such as Al, Ni and Nb is expected to be nearly isotropic while the mismatch between highly anisotropic materials such as Na is expected to have substantial variation with the orientation of the interface crack front. Thus, in estimating the variation of ε along a 3D interface crack front in anisotropic media, for fixed material orientations one may expand the bimaterial tensors such as **W** and **D** [related to Y_1 and Y_2 by (26)] as a Fourier series in the orientation angle of the crack front relative to crystal orientations in the interface plane. We do not pursue this point further here.

CONCLUSION

This paper is concerned with interfacial cracks in anisotropic elastic solids. The topic has been discussed by a number of authors previously, and controversies exist in that several different definitions for the crack-tip field have been proposed in the literature. We first devised a novel and convenient scheme for constructing interfacial crack fields and then carried out a mismatch analysis for understanding the oscillatory structure of the crack-tip stress singularity. The mismatch along a cracked interface ahead of the crack tip is analyzed via the SGF tensor of a homogeneous material, and is represented as a continuous distribution of dislocations whose superposed effect leads to the oscillatory crack-tip field. Among different definitions for the stress intensity factors for interfacial cracks, it is found that the solution proposed by WU (1990, 1991), which conforms to a general definition suggested by RICE (1988), is consistent with the analysis of local interface mismatch near the crack tip. We hope that the mismatch analysis can shed some light on the controversial issues from a different perspective.

To provide some more insight into the mismatch and oscillation at interfacial crack tips, the oscillation index ε has been numerically evaluated for two cases involving bonded graphite–epoxy and glass–epoxy fiber-reinforced composites with fiber directions misoriented across the interface plane. The results indicate that the oscillation index ε is on the order of a few hundredths, consistent with other related data reported in the past literature, and ε varies in an undulating fashion as a function of the crack orientation relative to fixed material coordinates. It is also demonstrated, by example using a group of crystals of cubic symmetry, that the tensor Im [**Y**] governing the interface mismatch can be conveniently expanded into a Fourier series as a function of the crack orientation angle with only a few significant Fourier coefficients.

Acknowledgement

H. G. acknowledges support from the NSF–MRL program through the Center for Material Research at Stanford University and a research initiation award from the IBM Corporation; M. A. and D. M. B. acknowledge support from the U.S. Department of Energy, Office of Basic Sciences, Division of Engineering, Mathematical, and Geosciences. We thank Professors T. C. T. Ting and J. R. Willis, and an anonymous reviewer, for their critical comments on an initial manuscript.

References

Bacon, D. J., Barnett, D. M. and Scattergood, R. O. 1979 In *Progresses in Materials Science* (edited by B. Chalmers, J. W. Christian and T. B. Massalski), Vol. 23, p. 51. Pergamon Press, New York.

Barnett, D. M. 1985 In *Structure and Deformation of Boundaries* (edited by K. A. Subramanian and M. A. Imam), p. 31. AIME.

Barnett, D. M. and Asaro, R. J. 1972 *J. Mech. Phys. Solids* **20,** 353.

Barnett, D. M. and Lothe, J. 1974 *J. Phys. F: Metal Phys.* **4,** 1618.

Barnett, D. M. and Lothe, J. 1975 *Phys. Norv.* **8,** 13.

Barnett, D. M. and Lothe, J. 1985 *Proc. R. Soc.* **A402,** 135.

Bassani, J. L. and Qu, J. 1989 *J. Mech. Phys. Solids* **37,** 434.

Clements, D. L. 1971 *Int. J. Engng Sci.* **9,** 257.

Eshelby, J. D., Read, W. T. and Shockley, W. 1953 *Acta Metall.* **1,** 251.

Gao, H. 1991 *J. appl. Mech.* **58,** 931.

Gotoh, M. 1967 *Int. J. Fracture Mech.* **3,** 253.

Hirth, J. P. and Lothe, J. 1982 *Theory of Dislocations*, 2nd edition, p. 836. John Wiley, New York.

Hutchinson, J. W. 1990 In *Metal–Ceramic Interfaces* (edited by M. Ruhle, A. G. Evans, M. F. Ashby and J. P. Hirth), p. 255. Pergamon Press, New York.

Ingebrigtsen, K. A. and Tonning, A. 1969 *Phys. Rev.* **184,** 942.

Kuo, C. M. and Barnett, D. M. 1991 In *Modern Theory of Anisotropic Elasticity and Applications* (edited by J. C. Wu, T. C. T. Ting and D. M. Barnett), p. 139. SIAM Publishers, Philadelphia, PA (in press).

Ni, L. and Nemat-Nasser, S. 1991 *J. Mech. Phys. Solids* **39,** 113.

Qu, J. and Bassani, J. L. 1989 *J. Mech. Phys. Solids* **37,** 417.

Qu, J. and Li, Q. 1991 *J. Elast.* **26,** 169.

Rice, J. R. 1988 *J. appl. Mech.* **55,** 98.

Rice, J. R., Suo, Z. and Wang, J. S. 1990 In *Metal–Ceramic Interfaces* (edited by M. Ruhle, A. G. Evans, M. F. Ashby and J. P. Hirth), p. 269. Pergamon Press, New York.

Stroh, A. N. 1958 *Phil. Mag.* **7,** 625.

Stroh, A. N. 1962 *J. math. Phys.* **41,** 77.

Suo, Z. 1990 *Proc. R. Soc.* **A427,** 331.

Tada, H., Paris, P. C. and Irwin, G. R. 1985 *The Stress Analysis of Cracks Handbook*. Del Research, Hellertown, PA.

Tewary, V. K., Wagoner, R. H. and Hirth, J. P. 1989 *J. Mater. Res.* **4,** 124.

Ting, T. C. T. 1986 *Int. J. Solids Struct.* **22,** 965.

TING, T. C. T. 1990 *J. Mech. Phys. Solids* **38,** 505.
TSAI, S. W. 1989 *Composite Design*, 4th edition. THINK COMPOSITES, Dayton, OH.
WILLIAMS, M. L. 1959 *Bull. seism. Soc. Am.* **49,** 199.
WILLIS, J. R. 1971 *J. Mech. Phys. Solids* **19,** 353.
WU, K. C. 1990 *J. appl. Mech.* **57,** 882.
WU, K. C. 1991 *Int. J. Solids Struct.* **27,** 455.